Journal of Chromatography A, 1218 (2011) 3718–3724

Contents lists available at ScienceDirect

Journal of Chromatography A

journal homepage: www.elsevier.com/locate/chroma

Utilizing a constant peak width transform for isothermal gas chromatography

Jeremy S. Nadeau, Ryan B. Wilson, Brian D. Fitz, Jason T. Reed, Robert E. Synovec*

Department of Chemistry, Box 351700, University of Washington, Seattle, WA 98195-1700, USA

ARTICLE INFO

Article history:
Received 15 October 2010
Received in revised form 24 January 2011
Accepted 1 April 2011
Available online 12 April 2011

Keywords:
Gas chromatography
Isothermal
Constant peak widths
Transform
Signal-to-noise ratio
High speed

ABSTRACT

A computational approach to partially address the general elution problem (GEP), and better visualize, isothermal gas chromatograms is reported. The theoretical computational approach is developed and applied experimentally. We report a high speed temporally increasing boxcar summation (TIBS) transform that, when applied to the raw isothermal GC data, converts the chromatographic data from the initial time domain (in which the peak widths in isothermal GC increase as a function of their retention factors, k), to a data point based domain in which all peaks have the same peak width in terms of number of points in the final data vector, which aides in preprocessing and data analysis, while minimizing data storage size. By applying the TIBS transform, the resulting GC chromatogram (initially collected isothermally), appears with an x-axis point scale as if it were instrumentally collected using a suitable temperature program. A high speed GC isothermal separation with a test mixture containing 10 compounds had a run time of ~25 s. The peak at a retention factor $k \sim 0.7$ had a peak width of ~55 ms, while the last eluting peak at $k \sim 89$ (i.e., retention time of ~22 s) had a peak width of ~2000 ms. Application of the TIBS transform increased the peak height of the last eluting peak 45-fold, and S/N ~20-fold. All peaks in the transformed test mixture chromatogram had the width of an unretained peak, in terms of number of data points. A simulated chromatogram at unit resolution, studied using the TIBS transform, provided additional insight into the benefits of the algorithm.

1. Introduction

Gas chromatography (GC) is a widely practiced chemical analysis technique, in particular for the analysis of volatile and semi-volatile compounds [1]. Over the years GC instrumentation has evolved in order to address the general elution problem (GEP), whereby temperature programming is commonly practiced, especially in the laboratory [2]. However, there are applications for GC in which temperature programming is neither widely practiced, nor readily engineered into a GC-analyzer to achieve sufficient precision and robustness. For example, with on-line process analysis applications of GC, isothermal GC is commonly practiced to provide a simpler, more robust chemical analyzer solution than temperature programmed GC [3]. Certainly, for high speed GC (e.g., separations on the order of a minute to sub-second timeframe), instrumentation for temperature programming has been successfully explored [4,5] and is commercially available for the 30 s to 1 min time frame [6,7]. However, it may be beneficial in many timely applications (e.g. remote monitoring, hand-held GC analyzers, and for on-line process monitoring), to be able to apply GC technology without the instrumental constraints of applying temperature programming (e.g. energy requirements to heat and cool the GC column), and simultaneously provide many of the benefits of addressing the GEP via a non-instrumental (i.e., computational) solution.

One suitable computational solution to addressing the GEP for isothermal GC is to apply a high speed temporally increasing boxcar summation (TIBS) transform to the raw isothermal GC data, in order to transform the data from the initial time domain (in which the peak widths in optimized isothermal open-tubular capillary GC increase as a function of their retention factor, k), to a transformed domain in which all peaks have the same peak width in terms of number of points in the final data vector. The TIBS transform is essentially an adaptation of well-known boxcar averaging [8–11], applied in a new way to isothermal GC data. By applying the TIBS transform, the resulting GC chromatogram (initially collected isothermally), appears as if it were instrumentally collected using an appropriate temperature program. Certainly, the resulting TIBS transformed chromatogram will not be able to cover as wide a boiling point range of eluting compounds as compared to a true temperature programmed chromatogram. However, the TIBS transformed chromatogram will be demonstrated to increase the signal-to-noise ratio (S/N) of the later eluting peaks [12], and via the increase in the relative peak height as a function of time may

* Corresponding author. Tel.: +1 206 685 2328; fax: +1 206 685 8665.
E-mail address: synovec@chem.washington.edu (R.E. Synovec).

0021-9673/$ – see front matter © 2011 Elsevier B.V. All rights reserved.
doi:10.1016/j.chroma.2011.04.007

improve the overall interpretability, or processing ability via eye or algorithm, of isothermal GC chromatograms. By improving the interpretability of isothermal GC chromatograms, the TIBS transform is complementary to the recently reported power transform method [13]. An example using previous data provides insight into the potential scope of applying the TIBS transform to high speed isothermal GC data. Based on our prior report in which we explored the peak broadening for very high speed GC (limited by the column band broadening and not off-column band broadening), the entire separation was only a few hundred ms, and the unretained peak had a width-at-the-base (W_b) of 5 ms at $k = 0$, and for a retained peak (at $k = 5$), the $W_b = 94$ ms [14]. Application of the TIBS transform would convert the peak at $k = 5$ to the same width as the $k = 0$ peak (in the transformed data point domain and not the initial time domain), and the peak height for the $k = 5$ peak would increase over 18-fold, making it much easier to inspect the chromatogram as a whole over a wide k range. Likewise, the S/N for the $k = 5$ peak could in principle increase by over 4-fold (i.e., $18^{1/2}$, assuming the baseline signal in the original time domain is governed by white noise).

In this report, the theory related to the basics of performing the TIBS transform is initially presented. For optimal implementation of high speed GC, peak broadening should be dictated by the on-column chromatographic processes, therefore off-column band broadening must be minimized from all sources, but in particular from the injection and detection processes. In this regard we implement herein a high-speed diaphragm valve (to inject ~25 ms sample pulses) and the FID, modified with a high-speed electrometer board to collect at 10,000 Hz (with data summed for analysis and initially stored at 200 Hz) [4,14]. We implement the single valve injection design for simplicity, and accept some off-column peak broadening due to injection at low k (0–1 range) allowing us to reduce the effective collection rate, hence the data size, to 200 Hz for analysis [4,14]. Application of fast Fourier transform (FFT) software [10,15,16], revealed limited line noise at high frequencies so FFT filtering was not performed. Calibration and implementation of the TIBS transform was performed with a test mixture using a 1 m × 100 μm i.d. capillary column operated near the minimum H per the Golay equation theory [17]. Isothermal temperature elution of the test mixture for calibration spanned a k range of ~0.7 to 89. The calibration was then applied to additional replicate runs of the test mixture to demonstrate reproducibility and overall feasibility. Issues such as chromatogram interpretability and S/N before and after applying the TIBS transform are explored and quantified to the extent possible. Simulated chromatograms were also generated in order to explore the concepts.

2. Theory

Excluding off-column sources of band broadening, the on-column band broadening, H, for an analyte with a retention factor of k as derived by Golay is given by

$$H = \frac{2D_{g,o}jf}{\bar{u}} + \frac{1 + 6k + 11k^2}{96(1+k)^2}\frac{d_c^2\bar{u}f}{D_{g,o}j} + \frac{2kd_f^2\bar{u}}{3(1+k)^2D_L} \quad (1)$$

where k is the retention factor of the analyte, d_c is the i.d. of the capillary, d_f is the thickness of the stationary phase film, $D_{g,o}$ is the diffusion coefficient of the analyte in the gas phase at the outlet of the column, j is the James-Martin gas compressibility factor, f is the Giddings gas compression correction factor, D_L is the diffusion coefficient of the analyte in the stationary phase, and $\bar{u}$ is the average linear flow velocity of the carrier gas. Since H is quantitatively the length variance per column length, L, of the analyte peak on-column, the appropriate translation to the detected peak width in units of time under isothermal conditions is given by (as previously derived [14]),

$$W_b = 4\sqrt{\frac{2D_{g,o}jf(1+k)^2t_o^2}{L^2} + \frac{(1+6k+11k^2)d_c^2ft_o}{96D_{g,o}j} + \frac{2kd_f^2t_o}{3D_L}} \quad (2)$$

where t_o is the dead time for the separation conditions. Generally, a linear relationship between peak width and retention factor k is generally observed for isothermal open-tubular capillary GC indicative of separation and overall peak broadening conditions that are dominated by the middle "mass transfer in the mobile phase" term of the Golay equation (specifically the $11k^2$ portion of the middle term, which makes W_b sufficiently linear with k per Eq. (12)) [14]. Hence, we anticipate the TIBS transform will be facilitated by a linear function. Putting this in a simplified general form for peak widths in units of time, yields the following,

$$W_{b,t} = m_t k + b_t \quad (3)$$

and the peak width in terms of number of points,

$$W_{b,p} = m_p k + b_p \quad (4)$$

Now, the boxcar width $W_{box}(k)$ for applying the TIBS transform is given by,

$$W_{box}(k) = \frac{W_{b,t}(k)}{W_{b,t}(k=0)} = \left(\frac{m_t k}{b_t}\right) + 1 \quad (5)$$

However, since $m_t/b_t = m_p/b_p$, then,

$$W_{box}(k) = \frac{W_{b,p}(k)}{W_{b,p}(k=0)} = \left(\frac{m_p k}{b_p}\right) + 1 \quad (6)$$

So, Eqs. (5) and (6) are equivalent, and either can be used to determine the width of the integrated boxcar window as a function of k with the initial chromatogram, however, the TIBS transform is ultimately applied to the data on the point scale axis. Whereas $W_{b,t}(k=0)$ is the width in units of time of the unretained peak, $W_{b,p}(k=0)$ is the width of the unretained peak in number of data points. Hence, $W_{b,p}(k=0)$ is a user selected minimum number of points to define a peak, and upon applying the TIBS transform, all peaks in the transformed chromatogram will have a width at $W_{b,p}$ ($k=0$). In practice, the user runs standards to determine the ratio m_p/b_p. As an example from prior work [14], this ratio was ~3, so based on Eq. (6), at $k=0$ the $W_{box} = 1$, and data stays as initially collected following the TIBS transform; and, at $k = 10$ the $W_{box} = 31$ and the data are summed with the resulting peak at this location increasing in signal 31-fold and the S/N increasing as much as $31^{1/2}$-fold if the baseline noise is limited by white noise. All peaks will have an equivalent peak width in terms of number of points. In this report, this number of points was found to be at $W_{b,p}$ ($k=0$) ~10 (at the data storage rate of 200 Hz for the unretained peak). However, the user is welcome to adjust this number as deemed satisfactory for a given application. Herein, Eq. (6) is determined via calibration, and applied to subsequent chromatograms.

3. Experimental

All chemicals were reagent grade or higher:hexane, anisole, octane, decane, butyl-benzene, undecane, naphthalene, dodecane (Aldrich, Fairlawn, NJ, USA), benzene, and chlorobenzene (Fischer Chemicals, Fairlawn, NJ, USA). Methane, used as a dead-time marker, was obtained from an in-house gas line (University of Washington, Seattle, WA, USA). A test mixture was prepared from these neat solvents. The ten solvents (components) were chosen such that peaks were well resolved and that the final eluting peak was barely visible above the baseline. Seven chromatograms of the test mixture were analyzed. Three of the chromatograms were used

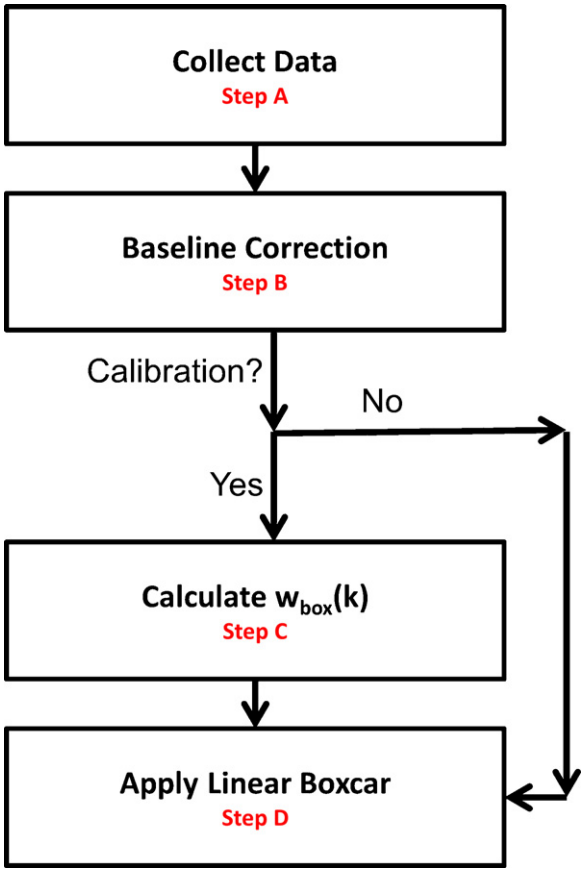

Fig. 1. The flow chart describes how the high speed temporally increasing boxcar summation (TIBS) transform is applied. The steps are labeled A–D for reference throughout this report. The function of retention time step, Step C, is only applied when the calibration data are run. At all other times, i.e., when the method is applied to a subsequent chromatogram, the TIBS transform is simply applied to the data using the stored calibration (Eq. (6)), skipping Step C.

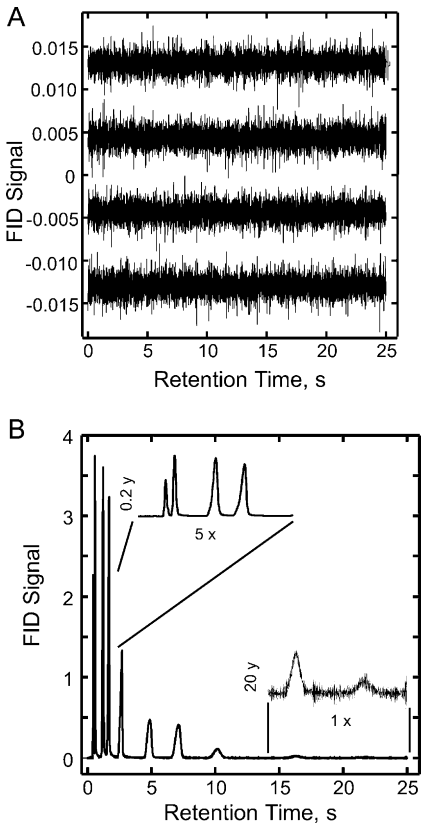

Fig. 2. (A) Four representative baseline noise files for a 30 s run. The noise level initially was at s_{noise} = 0.002 (standard deviation). (B) Representative test mixture isothermal chromatogram prior to applying TIBS transform. In the first few seconds of the separation, the analyte signals appear compacted together. However, at the end of the separation the analyte signals are spread out and the S/N is significantly decreased. The elution order is hexane, benzene, octane, chlorobenzene, anisole, decane, butyl-benzene, undecane, naphthalene, and dodecane. For the inset figures, the *x* and *y* axes are expanded and/or contracted as indicated.

for calibration, and four chromatograms for applying the calibration.

All chromatograms were obtained using an Agilent 6890 gas chromatograph with an auto-injector controlled by ChemStation software (Agilent Technologies, Palo Alto, CA, USA). The Agilent FID was supplemented with a custom electrometer that was built in-house and capable of providing data acquisition rate of 20 kHz. This electrometer was interfaced to a National Instruments data acquisition board (model PCI-MIO-16XE-50, National Instruments, Austin, TX, USA) and the resulting data was collected using a LabVIEW 8 (National Instruments) program written in-house at a rate of 10 kHz, and initially stored at 200 Hz. The GC instrument was modified to use a diaphragm valve (VICI, Valco Instruments Co. Inc., Houston, TX, USA), fitted with a 10 μl sample loop for injecting a sample volume onto the column. The single valve injection system presented by Hope et al. [18] was refined by face mounting the valve as described by Sinha et al. [19], allowing for a wider range of oven temperatures (comfortably to 250 °C). Valve injections were 25 ms. Valve timing and actuation were controlled using the same LabVIEW program described above. Sample was delivered from the GC inlet to the diaphragm valve via a 10 cm length of deactivated steel column with a 250 μm i.d. (UADTM-5, Quadrex Corporation, Woolbridge, CT, USA). This steel column transfer line was electrically insulated from the GC using two short lengths of deactivated fused silica column, also with 250 μm i.d. (10079, Restek, Bellefonte, PA, USA). The fused silica sections of the transfer line were coupled to the steel column using steel column unions with a 250 μm i.d. bore (VICI). A variable autotransformer (ISE, Inc, Cleveland, OH, USA) supplied ~12 V of alternating current to the transfer line via three high temperature electrical leads placed on opposite ends of the steel column unions, hence producing a heated transfer line leading to the diaphragm valve. Separations were completed using a 1 m Rtx-5 column (Restek) with a 100 μm i.d. and a 0.4 μm film thickness (5% phenyl/95% dimethyl polysiloxane). The absolute pressure at the head of the column was adjusted such that the dead time for an unretained peak (methane) was 240 ms. The overall analytical procedure for the data processing steps is outlined in Fig. 1, where the initial calibration and subsequent application of the TIBS transform is in Steps C and D. Prior to Steps C and D, the data are collected and processed with baseline correction, Steps A through B. Optimization of the S/N in isothermal chromatographic separations due to uniform signal averaging or boxcar is the major reason why the steps outlined in Fig. 1 improve the overall chromatogram interpretability and S/N after applying the TIBS transform to the collected data. The steps for applying the TIBS transform are identical when analyzing calibration chromatograms or subsequent chromatograms except for Step C. Step C is only run if the data are calibration samples. At that point, the peaks are identified automatically with a peak finding algorithm, the widths are calculated, and the width is calculated as a function of the retention times. This function is then transformed to find the boxcar window a function of retention time. Boxcar window as a function of retention time is the function, $W_{box}(k)$ in Eqs. (5) and (6),used in the linear transform for calibration chromatograms and subsequently transformed chromatograms in Step D. All data processing and simulations were performed using an in-house program writ-

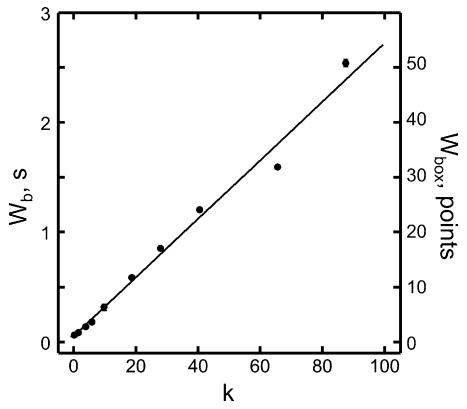

Fig. 3. The peak width as a function of retention factor, k, is used to produce the boxcar window size, $W_{box}(k)$ following Eqs. (5) and (6), needed to apply the TIBS transform. This function is produced in Step C in Fig. 1.

ten in Matlab 7.7.0(The Mathworks, Inc., Natick, MA, USA) and run on a personal computer equipped with an AMD Athlon 64 X2 4200+ 2.20 GHz processor and 3 GB of RAM operating under 64-bit Windows 7.

4. Results and discussion

We begin by evaluating baseline noise chromatograms and the calibration chromatogram data for the test mixture. After data are initially stored at 200 Hz for subsequent analysis, no filtering via FFT was necessary prior to applying the TIBS transform. The noise level of baseline blank runs with the same separation conditions as the calibration chromatograms show that the standard deviation of the noise is 0.002 V (Fig. 2(A)). The four noise files in Fig. 2(A) are offset for clarity.

In the early portion of the test mixture chromatogram (first few seconds of Fig. 2(B)), the peaks are tall and narrow with relatively higher S/N. As the retention time increases the peaks broaden under isothermal conditions. This broadening also decreases the peak height, thus decreasing the relative S/N of each individual peak. However, primarily the issue is often not S/N, but rather is one of difficulty in keeping all the peaks in a readily interpretable visual framework, since the peaks broaden so significantly from the beginning to the end of the isothermal separation. The retention factors, k, of these peaks range from 0.7 for the first eluting peak to 89 for the broad, initially almost unidentifiable dodecane peak at ~22 s. The last peak in the separation is initially near the limit of detection (LOD) in Fig. 2(B)). Looking at the chromatogram in Fig. 2B, it is apparent that following the chromatogram would benefit from

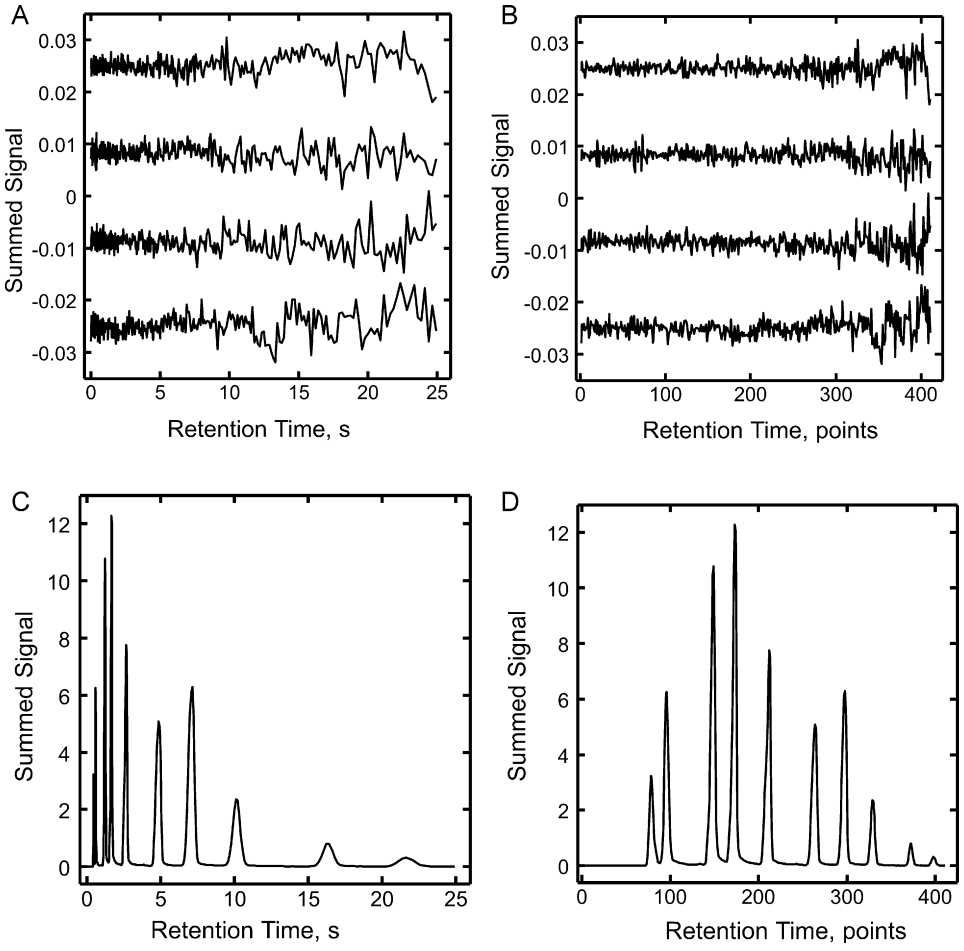

Fig. 4. (A) The TIBS transform has been applied via Fig. 3 to the baseline noise data (Fig. 2(A)) and is shown in the time domain. The noise level increases as the boxcar window increases. (B) The noise data are also shown in the constant TIBS data point domain. (C) The TIBS transform has been applied to a representative test mixture chromatogram (Fig. 2(B)). The data are shown in the time domain to show the changes in peak height as a function of time. This also shows that the time scale is no longer linear with the data points. (D) In the constant TIBS data point domain, the peaks now appear as if separated via a temperature program, with constant peak width and improved sensitivity at the higher retention times.

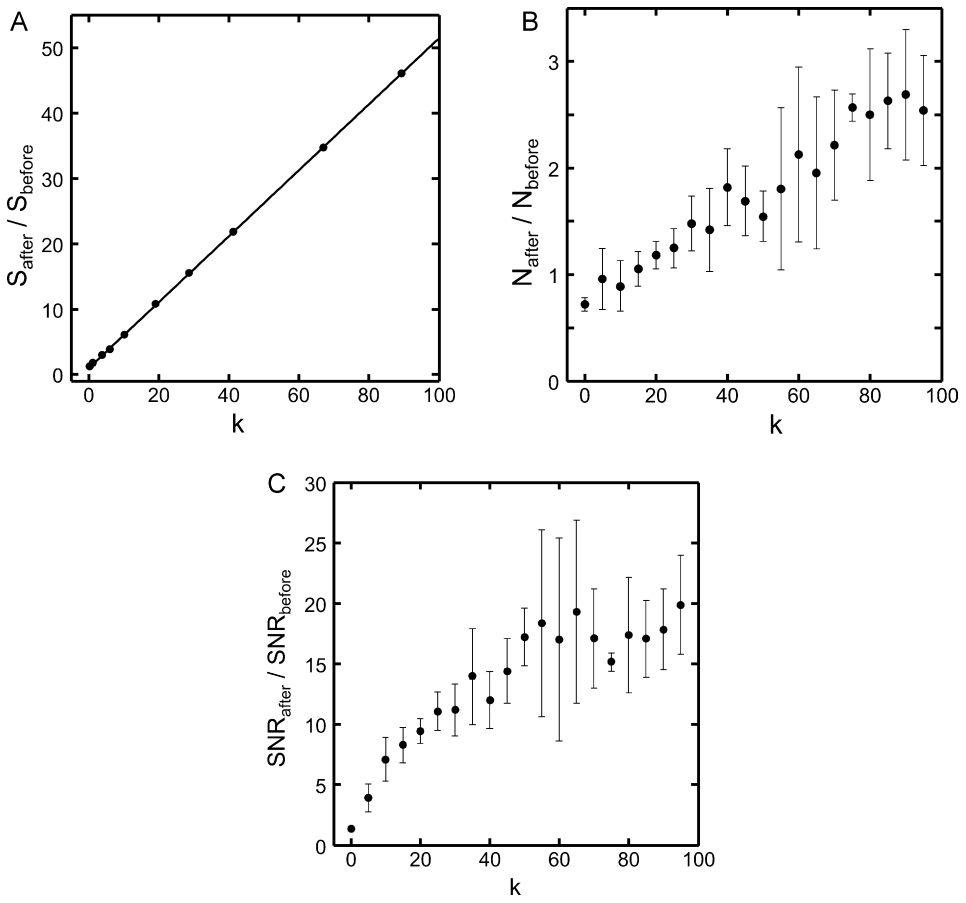

Fig. 5. (A) Relative peak heights for each analyte in four replicate trials with (i.e., after) and without (i.e., before) the TIBS transform applied to the test mixture (i.e., replicates of Figs. 2(B) and 4(C)). (B) Relative noise for evenly distributed retention factor intervals in four replicate trials after and before the TIBS transform applied to baseline noise (i.e., replicates of Figs. 2(A) and 4(A)). (C) Relative S/N, where SNR refers to signal-to-noise ratio in the axes label, for each retention factor interval in four replicate noise data divided into the equivalent intervals on the line for the relative signal (A) after and before the TIBS transform applied (i.e., the ratio of results in (A) to (B)).

application of the TIBS transform that will yield peaks of constant width throughout, and hence, dramatically benefit the interpretation of the overall chromatogram by rendering the later eluting peaks with significantly higher peak heights than they initially exhibit in Fig. 2(B). At this stage the test mixture chromatogram (Fig. 2(B)) is ready to be developed by the TIBS transform.

For the calibration procedure, Step C, Fig. 1, three chromatogram replicates like that in Fig. 2(B) were used. The peak width data from chromatograms such as Fig. 2(B) provides the basis for the TIBS transform, in which the peak widths (in units of time) following Eq. (3) are plotted as a function of k. Additionally, the boxcar window size $W_{box}(k)$ following Eqs. (5) and (6) is provided on the right side of the y-axis. Hence, Fig. 3 shows Step C of Fig. 1. Because the peak widths are essentially linear as a function of k (see discussion following Eq. (2)), then the best fit linear function in Fig. 3 that relates $W_{box}(k)$ to k can be used to calculate the TIBS transform function. For the data in Fig. 4 the ratio m_p/b_p in Eq. (6) was determined to be 0.5. For example, with this data the $W_{box}(k)$ begins at a value of 1 ($k = 0$) and grows to 45 for the last eluting peak in the test mixture chromatogram ($k = 89$).

The calibration from Fig. 3 was then applied to baseline noise data (i.e., Fig. 2(A)). The result of applying the TIBS transform on Fig. 2(A) baseline noise data is shown in Fig. 4(A). The noise data are displayed in the time domain initially to show that not only is the data rate decreasing as a function of time, but that the noise level is increasing in the same time domain. Displaying the data in the TIBS transformed domain (Fig. 4B), i.e., plotting as a function to retention time in points on the x-axis, more clearly shows how the noise level is increasing as the box size is increased. The noise does increase using the TIBS transform, as expected. Likewise, the calibration from Fig. 3 was applied to four replicates of the test mixture chromatogram (i.e., one of them being the chromatogram in Fig. 2(B)). The result of applying the TIBS transform on Fig. 2(B) test mixture chromatogram is shown in the time domain in Fig. 4(C). Clearly, each peak from Fig. 2(B) with a boxcar size larger than 1 (Fig. 3) increases in height without changing it's width in time (Fig. 4C). As expected and desired, in the TIBS transform domain, all peaks have essentially the same width (in numbers of points) in Fig. 4(D) chromatogram. It is interesting to note that the linear increase in the boxcar window causes the time units to increase non-linearly throughout the separation (Fig. 4(B) and (D)). Although qualitative in nature, the chromatogram in Fig. 4(D) is easier to visually inspect compared to Fig. 2(B), since all peaks have the same width and the later eluting peaks have been "magnified" due to the TIBS transform effect. Although resolution has not been changed by the TIBS transform, the peaks are also spaced apart analogous to a temperature program, and this is also desirable for ease of interpretation. As a summary of the performance of the TIBS transform with the test mixture chromatogram and baseline noise chromatogram, the plots in Fig. 5(A)–(C) provide quantitative results for the relative peak heights (Fig. 5(A)), relative noise (Fig. 5(B)), and relative S/N (Fig. 5(C)). From Fig. 5(A) we see that the relative peak heights increased by a factor of ~45 (at $k = 89$) for post to prior the TIBS transform. As expected the noise also increases,

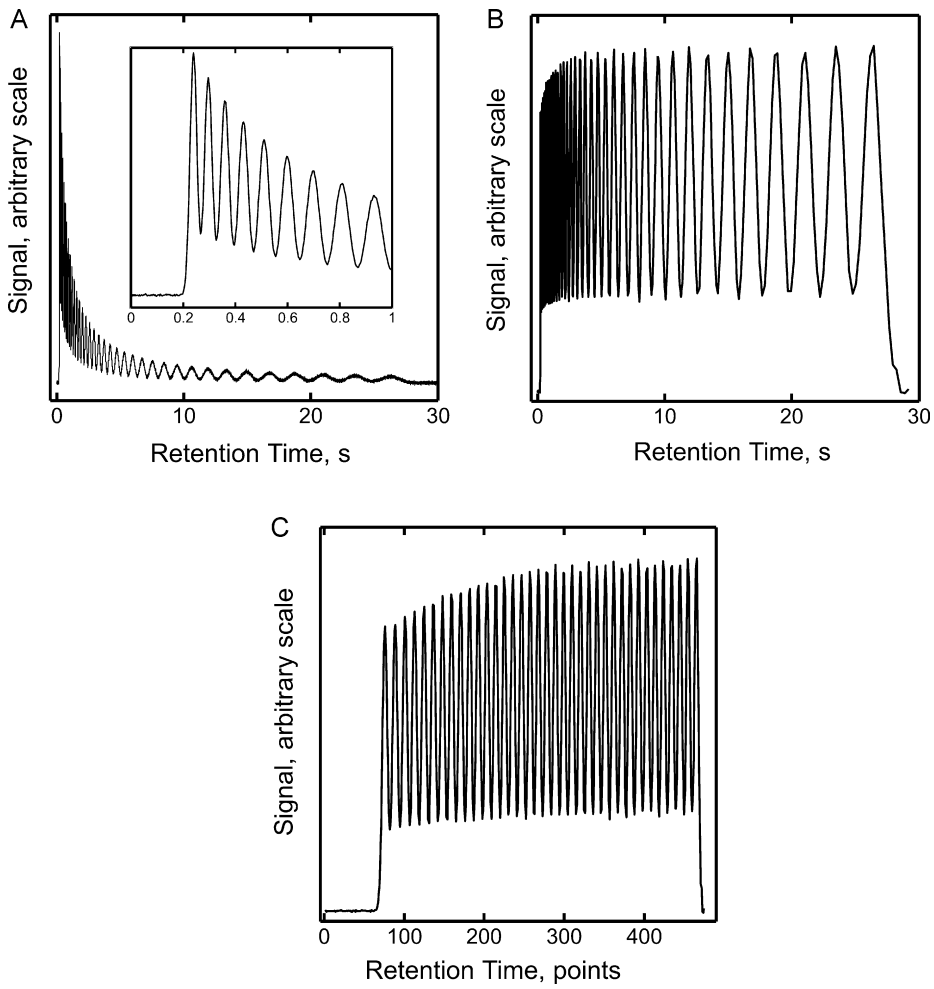

Fig. 6. (A) Simulated isothermal chromatogram in which all peaks have equal area and a unit resolution. The simulation is based on the data and $W_{box}(k)$ from Fig. 4. (B) Application of the TIBS transform improves the interpretability of the chromatogram of the later eluting peaks in the time domain and (C) the earlier eluting peaks in the constant TIBS data point domain.

so in Fig. 5(B) we see that the relative noise increased by a factor of ~2.5(at $k = 89$). By taking the ratio of the results from the line in Fig. 5(A) and (B), the relative S/N was obtained as shown in Fig. 5(C). A satisfactory ~20-fold improvement in S/N was achieved at $k = 89$ using the TIBS transform, albeit with this data set and instrumental performance (other detection systems may fare either better or worse). The general trend in Fig. 5(C) is a square root dependence on the TIBS boxcar size, which is indicative that the noise did exhibit a significant level of randomness, although was not totally "white" in nature. The primary benefits of using the TIBS transform remain the increase in S/N and sensitivity (Fig. 5(A)), and more straightforward interpretability (Fig. 4(D) relative to Fig. 2(B)). Another potential benefit is that many chemometric algorithms and retention time alignment algorithms benefit significantly from having peaks of uniform peak width, however additional study of this idea is warranted.

To further highlight the potential interpretation of isothermal separations, an isothermal chromatogram with peaks of equivalent areas was simulated based on the data in Fig. 3, with the simulated chromatogram presented in Fig. 6(A). Retention times and peak widths were iteratively calculated such that adjacent peaks were separated by unit resolution throughout and then simulated white noise added to the chromatogram. For a run time of a little less than 30 s (similar to that of the test mixture chromatogram used for calibration) the peak capacity is 40, with the last peak having a $k = 110$. The peak height decreases by a factor of 40 between the first and last peak while the peak width increased by a factor of 41. Application of the TIBS transform to this simulated isothermal chromatogram makes all 40 peaks essentially equal in height in the time domain (Fig. 6B), and equal height and width (Fig. 6(C)) in the data point domain. The increase in noise as the boxcar size increases over the k range, causes the peak heights to deviate slightly from perfectly equivalent. This deviation is clearer in Fig. 6(C). In comparing the before and after transform chromatograms it is apparent a comparison can be made between the TIBS transform and temperature programmed GC. Despite the unchanged peak capacity, the TIBS transform, like temperature programming, improves peak height and width (if plotted in the x-axis data point domain) for later eluting compounds while maintaining the resolution of the early eluting compounds. Additionally, it is envisaged that the TIBS transform would be useful in preprocessing algorithms, like chromatographic alignment, and peak identification algorithms. Indeed, chromatographic retention time alignment, typically uses a segment size or window size parameter that is approximately equal to the peak width. By adjusting to a constant peak width domain using TIBS, the user can optimize this parameter much simpler and faster.

5. Conclusions

A computational algorithm, the TIBS transform, is presented and experimentally demonstrated, providing a means to produce nearly

constant peak widths for isothermal GC. The TIBS transform may be useful for GC applications in which temperature programming is either not as popular, or readily engineered into a GC-analyzer to achieve sufficient precision and robustness, e.g., with on-line process analysis with GC, isothermal GC is commonly practiced to provide a simpler, more robust chemical analyzer solution than temperature programmed GC.

References

[1] F.L. Dorman, J.J. Whiting, J.W. Cochran, J. Gardea-Torresdey, Anal. Chem. 82 (2010) 4775.
[2] W.E. Harris, H.W. Habgood, Programmed Temperature Gas Chromatography, J. Wiley, New York, 1966.
[3] N.E. Watson, M.M. VanWingerden, K.M. Pierce, B.W. Wright, R.E. Synovec, J. Chromatogr. A 1129 (2006) 111.
[4] V.R. Reid, A.D. McBrady, R.E. Synovec, J. Chromatogr. A 1148 (2007) 236.
[5] V.R. Reid, M. Stadermann, O. Bakajin, R.E. Synovec, Talanta 77 (2009) 1420.
[6] J. Dalluge, R. Ou-Aissa, J.J. Vreuls, U.A.Th. Brinkman, J.R. Veraart, J. High Resolut. Chromatogr. 22 (1999) 459.
[7] A. Grall, C. Leonard, R. Sacks, Anal. Chem. 72 (2000) 591.
[8] D.C. Harris, Quantitative Chemical Analysis, W.H. Freeman, New York, 1999.
[9] G.M. Hieftje, Anal. Chem. 44 (1972) A69.
[10] D.L. Massart, Handbook of Chemometrics and Qualimetrics, Elsevier, Amsterdam, 1997.
[11] D.A. Skoog, F.J. Holler, T.A. Nieman, Principles of Instrumental Analysis, Brooks/Cole, Pacific Grove, 1997.
[12] R.E. Synovec, E.S. Yeung, Anal. Chem. 57 (1985) 2162.
[13] R.A. Shalliker, P.G. Stevenson, D. Shock, M. Mnatsakanyan, P.K. Dasgupta, G. Guiochon, J. Chromatogr. A 1217 (2010) 5693.
[14] G.M. Gross, B.J. Prazen, J.W. Grate, R.E. Synovec, Anal. Chem. 76 (2004) 3517.
[15] G.M. Hieftje, Anal. Chem. 44 (1972) A81.
[16] L. Pasti, B. Walczak, D.L. Massart, P. Reschiglian, Chemom. Intell. Lab. Syst. 48 (1999) 21.
[17] V.R. Reid, J.A. Crank, D.W. Armstrong, R.E. Synovec, J. Sep. Sci. 31 (2008) 3429.
[18] J.L. Hope, K.J. Johnson, M.A. Cavelti, B.J. Prazen, J.W. Grate, R.E. Synovec, Anal. Chim. Acta 490 (2003) 223.
[19] A.E. Sinha, K.J. Johnson, B.J. Prazen, S.V. Lucas, C.G. Fraga, R.E. Synovec, J. Chromatogr. A 983 (2003) 195.